JOURNAL OF THERMOPHYSICS AND HEAT TRANSFER
Vol. 16, No. 2, April–June 2002

Shock Standoff on Hypersonic Blunt Bodies in Nonequilibrium Gas Flows

George R. Inger,* Charlotte Higgins,† and Richard Morgan‡
University of Queensland, Brisbane, 4072 Australia

This paper presents a new theory of hypersonic blunt-nose shock standoff, based on a compressibility coordinate transformation for inviscid flow. It embraces a wide range of nonequilibrium shock-layer chemistry and gas mixtures including ionization and freestream dissociation. An extended binary scaling property of the analysis is also demonstrated. Specific application is made here to the family of arbitrarily diluted dissociating diatomic gases, with parametric study results presented for the scaled shock standoff distance as a function of an appropriate blunt-nose region Damköhler number. Comparisons with other theories and data in the case of nitrogen are also given and discussed.

Nomenclature

A, A_2	=	atom, molecule, respectively
C	=	constant in dissociation rate relation, Eq. (14)
c_j	=	mass fraction of jth specie
f	=	mass fraction of dilutent
h_D	=	dissociation energy per unit mass
I	=	integral property, Eq. (15)
J	=	dimensionality index, Eq. (1)
J_v, J_R	=	indices denoting vibrational or rotational internal energy, respectively, Eq. (12)
K	=	nondimensional dilution parameter, Eq. (10)
K_{EQ}	=	equilibrium constant, Eq. (9)
k_D, k_R	=	dissociation, recombination rate coefficients, respectively
ℓ	=	$\rho(1-\varepsilon_F)/\rho_F$
M	=	Mach number
M_j	=	molecular weight of jth specie
p	=	static pressure
R_B	=	nose radius
R_u, R_{A2}	=	universal and molecular specie gas constants, respectively
T	=	absolute static temperature
T_D	=	characteristic dissociation temperature (h_D/R_{A2})
U, V	=	velocity components parallel and normal to the body, respectively
U_∞	=	freestream (flight) velocity
$\dot{w}_\alpha$	=	net rate of atomic specie mass production caused by gas phase chemical reaction
x, y	=	coordinates parallel and normal to the body, respectively (Fig. 1)
α	=	degree of dissociation
β_s	=	effective stagnation point velocity gradient
Γ_D	=	shock-layer Damköhler number, Eq. (14)
γ	=	specific heat ratio
$\tilde{\Delta}$	=	density-scaled standoff distance, Eq. (16)
δ_S	=	standoff distance at the body nose (Fig. 1)
ε_F	=	density ratio ρ_∞/ρ_F based on frozen shock-layer flow conditions
η	=	density-scaled shock layer y coordinate, Eq. (2)
θ	=	T/T_D
λ	=	$k/\mathrm{Arc}\sin k$ with $k=\sqrt{(1-3\varepsilon_F)}/\sqrt{(3\varepsilon_F)}$ for $J=0$; $=[1+\sqrt{(8\varepsilon_F/3)}]/\sqrt{(8\varepsilon_F/3)}$ for $J=1$
ρ	=	mixture density
τ_D	=	$U_\infty^2/2(1-f)h_D$
Ω	=	postshock relaxation Damköhler number, Eq. (17)

Subscripts

EQ	=	equilibrium-dissociated shock-layer conditions
F	=	chemically-frozen shock layer conditions
REF	=	reference properties in chemical rate formulae, Eq. (9)
S	=	stagnation properties
∞	=	freestream conditions

Introduction

THE standoff distance of the bow shock in the stagnation region of a blunt body (Fig. 1) is known to be sensitive to the thermochemical state within the underlying shock layer[1] and hence an important flowfield observable in modern hypervelocity test facilities.[2] It is, therefore, useful to have a fundamentally based theory for predicting and correlating data for shock standoff, which embraces a wide range of nonequilibrium shock-layer conditions involving both dissociating and ionizing gas mixtures.

Exact numerical solution codes are of course currently available to serve this need; however, such purely computational fluid dynamics (CFD) tools are expensive to use for engineering parametric studies and in any case do not readily yield the physical insight and similitude laws needed for experimental design and data interpretation. On the other hand, the existing approximate analytical methods, such as those based on crude average shock-layer density concepts, may not bear the weight of the desired extension to include arbitrary dissociation and multitemperature ionization. To improve this situation, the present paper describes the formulation of a new analytical theory of hypersonic, blunt-nose shock standoff based on the use of a compressibility coordinate transformation method for inviscid shock-layer flow, which embraces a wide range of nonequilibrium shock-layer chemistry and gas mixtures including ionization and arbitrary degrees of freestream dissociation. It is shown that the resulting theory also possesses an extended binary scaling property that is very useful in the design of simulation facilities for high altitude hypervelocity flight. As the first step in exploring the theory, we apply it here to the specific but very important family of dissociating diatomic gases that are diluted by an arbitrary amount of any desired inert dilutant (such application is especially important

Presented as Paper 2001-0812 at the AIAA 39th Aerospace Sciences Meeting, Reno, NV, 8–11 January 2001; received 30 January 2001; revision received 21 April 2001; accepted for publication 22 May 2001.

*Visiting Professor, Centre for Hypersonics; currently Professor, Department of Aerospace Engineering and Engineering Mechanics, 2239 Howe Hall, Iowa State University, Ames, IA, 50011. Associate Fellow AIAA.
†Graduate Research Student, Centre for Hypersonics.
‡Director, Centre for Hypersonics.

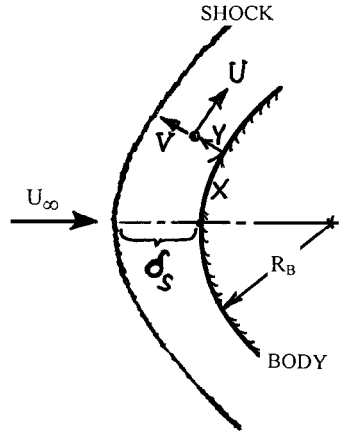

Fig. 1 Schematic of blunt-body stagnation flow region.

in regard to planetary entry studies in the University of Queensland superorbital facilities[3]).

The detailed Damköhler similitude and numerical results for the shock standoff distance and associated shock-layer properties are presented and discussed for the specific cases of dissociating nitrogen and diluted hydrogen[4] (with neon or helium), including the examination of the effect of a newly defined dilution parameter. The influence of the molecular vibrational energy excitation level is also considered. Comparisons of the present theory with experimental data obtained in nitrogen supporting our approach are given as well.

Theoretical Formulation

An approximate analytical description of the inviscid shock standoff problem for a two-dimensional or axisymmetric blunt-nose region at zero angle of attack has been formulated under the following assumptions (Fig. 1):

1) The postshock static pressure is a known constant across the shock layer.

2) The tangential velocity component is of the form $U \approx \beta_S x$, where β_S is a known constant across the shock layer equal to the effective stagnation point velocity gradient dU_e/dx that accounts for the influence of the $U(y)$ variation across the shock layer on conditions right behind the shock.

3) Low-Reynolds-number viscous shock-layer effects are negligible as regards their influence on standoff distance.

For hypersonic continuum flow at shock-layer Reynolds numbers above 3×10^2 (which pertains to most anticipated applications), these assumptions[5] are known to provide an acceptable basis for describing the aerothermochemical aspects of the nonequilibrium inviscid shock-layer flow in the immediate vicinity of the stagnation line $x \to 0$, yielding a prediction of chemistry-sensitive shock standoff distance δ_S that is well within the accuracy of measurement in any known or contemplated experimental scheme/hypervelocity simulation facility combination.

Regardless of the type of gas or its detailed specific chemistry, the foregoing assumptions immediately provide the following solution for the normal velocity component V in terms of the shock-layer density variation $\rho(y)$ by virtue of continuity:

$$\rho(y)V(y) = -(1+J)\beta_S \int_0^y \rho \, dy \tag{1}$$

where $J = 0, 1$ for two-dimensional or axisymmetric flow, respectively, and where ρ and V are functions of y only (upon excluding terms of order x^2) by virtue of symmetry about $x = 0$. In general Eq. (1) yields a nonlinear variation of V across the shock layer; only in the constant density approximation (which is not made here), such as pertains to either the fully equilibrium or fully chemically frozen limit, does the V variation become linear.

A Howarth–Dorodnitsyn type of compressibility transformation is now introduced in the normal coordinate to exploit Eq. (1). Specifically, preliminary study shows that it is advantageous to introduce the density-stretched coordinate η defined by

$$\eta \equiv (1+J)\frac{\beta_S R_B}{U_\infty}\int_0^y \frac{\rho}{\rho_\infty} d\left(\frac{y}{R_B}\right) \tag{2}$$

to enable application of conservation of mass across the shock in the simplest form. Equation (1) now yields the simple nondimensional analytical form

$$\rho V = -\rho_\infty U_\infty \eta \tag{3}$$

Equation (3) offers several advantages. First, it shows that the mass flux per unit area (or $\rho \cdot V$ product) varies linearly with η across the shock layer, which simplifies the analysis of the species conservation equation as will be shown next. Second, the location of the shock in the η coordinate now becomes especially convenient because $\rho V = -\rho_\infty U_\infty$ must be true in the gas right behind the shock to satisfy mass conservation across each unit area patch of the shock; we see from Eq. (3) that $\eta = 1$ is the shock location in the transformed coordinate regardless of the chemistry or dimensionality of the flow. This latter feature immediately provides a key result in the form of a general working relationship for calculating the physical shock standoff distance δ_S; inverting the transformation of Eq. (2) using Eq. (3) gives

$$(y)_{\eta=1} \equiv \delta_S = \frac{U_\infty}{\beta_S(1+J)}\int_0^1 \frac{\rho_\infty}{\rho} d\eta \tag{4}$$

Equation (4) shows that once the density profile is solved in the η coordinate using the species conservation and energy conservation equations plus the equation of state one integration immediately yields the shock standoff distance. This equation further reveals an appropriate nondimensional form for expressing δ_S:

$$\frac{\delta_S}{R_B} = \left(\frac{U_\infty}{\beta_S R_B}\right)\frac{\int_0^1 (\rho_\infty/\rho)\, d\eta}{(1+J)} \tag{5}$$

which is particularly convenient because the nondimensional group $\beta_S R_B/U_\infty$ is known to depend essentially only on the frozen shock-layer density ratio.[6,7] Finally, because the integral is only weakly dependent on J in nonequilibrium flow Eq. (5) correctly predicts that the three-dimensional relief effect reduces δ_S relative to the two-dimensional ($J = 0$) case.

We complete our exploration of the consequences of using a compressibility transformation by examining its effect on formulating the species conservation equation. For any chemical process involving the net formation of a species mass fraction α, we have in the immediate neighborhood of the stagnation line (neglecting diffusion) that

$$\rho V \frac{d\alpha}{dy} = \dot{w}_\alpha \tag{6}$$

where $\dot{w}_\alpha$ is the net rate of species mass formation per unit volume caused by whatever gas phase chemistry scheme is under consideration. Then applying Eqs. (2) and (3), Eq. (6) becomes the following in the η coordinate:

$$\eta\frac{d\alpha}{d\eta} = \frac{-(\dot{w}_\alpha/\rho)}{(1+J)\beta_S} = \frac{-R_B/U_\infty(\dot{w}_\alpha/\rho)}{(1+J)(\beta_S R_B/U_\infty)} \tag{7}$$

This expression is obviously much more tractable as regards the left-hand side convective derivative aspect, whereas the right-hand side chemistry term is now in an appropriate nondimensional form because both $\dot{w}_\alpha/\rho$ and U_∞/R_B have the same units of reciprocal time.

Application to Diluted Dissociating Diatomic Gas Mixtures

We now consider the specific case of a diatomic gas diluted by a mass fraction f of some arbitrary inert monatomic gas (e.g., helium or neon), which undergoes the dissociation-recombination reaction

$$A_2 + M \underset{k_R}{\overset{k_D}{\rightleftharpoons}} 2A + M \tag{8}$$

where M is any third body (A_2, A, or inert gas). Then, according to the law of mass action combined with the principle of detailed balancing and the use of the usual mole-mass fraction relationship, the net rate of change of atomic species mass per unit volume caused by Eq. (8) is

$$\dot{w}_\alpha = \frac{\rho^2}{2}(1-f)\sum_{j=A_2,A,f}\frac{c_j k_{Dj}}{M_j} \times \left[\underbrace{1-\alpha}_{\text{Dissociation}} - \underbrace{\frac{4\rho(R_u/M_{A2})T(1-f)\alpha^2}{K_{\text{EQ}}(T)}}_{\text{Recombination}}\right] \tag{9}$$

where the c_j are mass fractions [$c_A = (1-f)\alpha$, $c_{A2} = (1-f)(1-\alpha)$], and the equilibrium parameter K_{EQ} takes the form $K_{\text{EQ}} = p_{\text{REF}}(T/T_{\text{REF}})^s e^{-(TD/T)}$ in terms of the known parameters p_{REF}, T_{REF}, s, and the characteristic dissociation temperature T_D of the type of diatomic gas under consideration.

The mixture density ρ of such a reacting gas can be expressed in terms of α and the temperature T (here assumed the same for all species) by the equation of state, which upon use of Dalton's law becomes

$$p = \rho(R_u/M_{A2})T(1-f)(1+\alpha+K) \tag{10}$$

where $K \equiv fM_{A2}/(1-f)M_f$ is a new nondimensional dilution parameter that will also appear subsequently in the energy equation. The use of Eq. (10) in Eq. (9) provides the desired reaction rate term on the right side of the species conservation Eq. (7); upon taking each k_{Dj} to be adjusted to the same activation energy and substituting $P \approx \rho_\infty U_\infty^2(1-\varepsilon_F)$ and $\beta_S R_B/U_\infty \approx \sqrt{[2\varepsilon_F(1-\varepsilon_F)]\lambda}$ from constant density shock-layer/Newtonian theory,[8] Eq. (7) becomes

$$\eta\frac{d\alpha}{d\eta} = \frac{-k_{\text{DA2}}\rho_\infty R_B U_\infty}{2(1+J)R_u T}\sqrt{\frac{(1-\varepsilon_F)}{2\varepsilon_F}}\left\{1+\left[2\left(\frac{k_{\text{DA}}}{k_{\text{DA2}}}\right)-1\right]\alpha + K\frac{k_{\text{Df}}}{k_{\text{DA2}}}\right\}(1+\alpha+K)^{-1}\left\{(1-\alpha)-\left[\frac{4\rho R_{A2}(1-f)T}{K_{\text{EQ}}}\right]\alpha^2\right\} \tag{11a}$$

where we employ for the dissociation rate the value

$$k_{\text{DA2}} \equiv CT^N e^{-T_D/T} \tag{11b}$$

Our formulation is completed by providing the energy conservation equation governing the mixture temperature T. For the steady, adiabatic, nonradiating shock layer under consideration, the total enthalpy $h + V^2/2$ is constant; for hypersonic flows with high density shock layers and $U_\infty^2 \gg 2R_{A_2}T_\infty$, this leads to the algebraic relation that

$$\alpha + \tfrac{5}{2}(T/T_D)\left[1+\alpha+K+\tfrac{2}{5}(1-\alpha)(J_R+J_V)\right] \approx \left[U_\infty^2/2(1-f)h_D\right] + \alpha_\infty \tag{12}$$

where $h_D \equiv R_{A2}T_D = R_u T_D/M_{A2}$ and J_R, J_V are indices that indicate the fraction of classical rotational or vibrational internal molecular energy assumed to be activated (e.g., $J_R = J_V = 1$ for complete activation of both, $J_R = 1$ but $J_V = 0$ for negligible vibration, and $J_R = 1$ but $J_V = \frac{1}{2}$ for the well-known Lighthill ideal dissociating gas model). In the present high-density shock-layer application to H_2, notwithstanding its 100-fold slower rotational relaxation time compared to N_2, we shall assume that full rotational excitation ($J_R = 1$) still occurs before the onset of dissociation.

Similitude Properties and Binary Scaling

The foregoing formulation indicates that the proper scaling of the shock property distributions is not the actual physical distance normal to the body but rather the density-stretched variable η. Moreover, inspection of the governing Eqs. (10–12) reveals that these properties obey the following general similitude law for all types of diluted dissociating diatomic gas mixtures:

$$\alpha(\eta), \theta(\eta), \ell(\eta) = f_{\text{ns}}\left[\Gamma_D, \tau_D, K, \alpha_\infty, \frac{(1-\varepsilon_F)\rho_\infty}{\rho_{\text{REF}}}\right] \tag{13}$$

where $\theta \equiv T/T_D$, $\ell \equiv \rho/\rho_\infty(1-\varepsilon_F)$ and $\tau_D \equiv U_\infty^2/2(1-f)h_D$ with the uninteresting $f = 1$ limit excluded. Here $\rho_{\text{REF}} \equiv \rho_{\text{REF}}M_{A2}(T_D/T_{\text{REF}})^S/R_u T_D$ and Γ_D is the dissociation Damköhler number appropriate to a blunt nose defined by

$$\Gamma_D \equiv \frac{CT_D^{N-1}R_B(1-\varepsilon_F)\rho_\infty U_\infty}{2(1+J)R_u\sqrt{2\varepsilon_F(1-\varepsilon_F)}} \tag{14}$$

Note that the last parameter on the right side of Eq. (13) derives from the recombination rate term of Eq. (9). The corresponding scaling law governing the shock standoff distance, which is the integrated effect of the shock-layer properties, is that

$$(1+J)\frac{\delta_S}{R_B}(1-\varepsilon_F)\sqrt{2\varepsilon_F(1-\varepsilon_F)} = \int_0^1 \ell^{-1}(\eta)\,d\eta \equiv I\left[\Gamma_D, \tau_D, K, \alpha_\infty, \frac{(1-\varepsilon_F)\rho_\infty}{\rho_{\text{REF}}}\right] \tag{15}$$

which we may note includes on the left side the blunt-body scaling factor identified previously by Stalker.[6]

Although the practical utility of the general similitude of Eq. (13) is rather limited, it takes on greater importance in those high-altitude/hypervelocity regimes of flight where the effect of recombination in the nonequilibrium chemistry is negligible and the last parameter of Eqs. (13) and (15) drops out of consideration. Under such an approximation the nondimensional shock-layer profiles for a given α_∞ in a particular type of gas mixture at any fixed flight velocity U_∞ (and hence τ_D) depend only on the Damköhler number τ_D and so form a distinct parametric family of curves as indicated in Fig. 2.

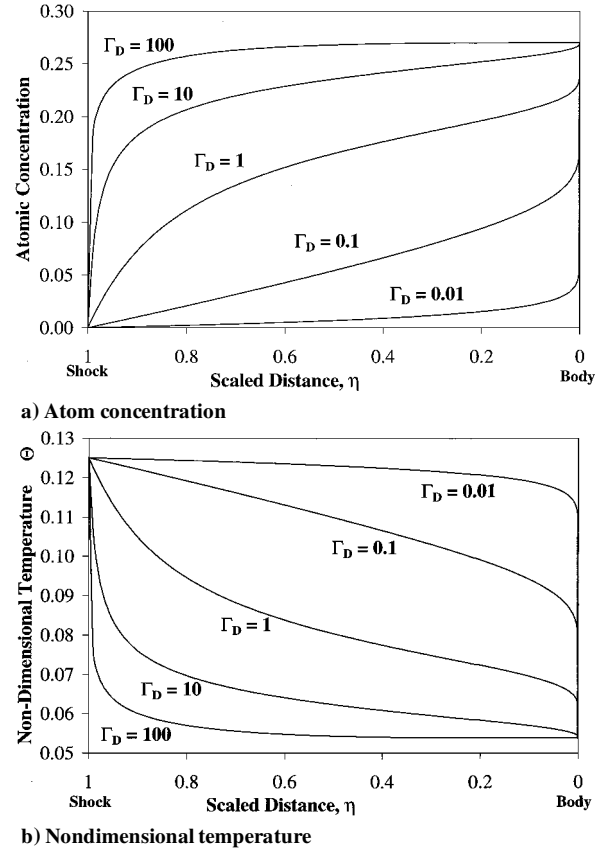

Fig. 2 Typical flow property distributions across the shock layer on spheres in dissociated nitrogen ($T_\infty = 1000$ deg, $\alpha_\infty = 0$, $\tau_D = 0.50$).

This is the generalized binary scaling property of the present theory, wherein appropriate nondimensional physical properties scaled in terms of the density-stretched variable η depend only on the value of Γ_D for given α_D and τ_D. A particular version of this binary scaling in which scaled properties remain the same for a fixed $\rho_\infty \cdot R_B$ [see Eq. (14)] has in fact been used for some time[9] to simulate nonequilibrium flows around large full-scale flight bodies by testing smaller models at higher densities in ground-based wind-tunnel facilities.

Parametric Studies

In this section we present the results of a systematic study of the present theory showing the influence of the various similitude parameters on the nondimensional standoff distance. Typical shock-layer distributions of atomic concentration and temperature resulting from the solution of Eqs. (11) and (12), used to obtain the density integral involved in the standoff determination (Eq. 15), are presented in Figs. 2a and 2b. In obtaining these profiles and the results that follow, the chemical kinetic data of Park[10] has been used along with the assumption that $\gamma_F = \frac{8}{6}(J_v = \frac{1}{2})$.

Damköhler-Number Correlation

The Damköhler number Γ_D is obviously of dominating importance in assessing the influence of departures from shock-layer dissociative equilibrium on shock standoff distance. Examination of the Γ_D effect also proves to be a revealing way to compare the present theory against existing theories and available experiments.

Figure 3 shows predictions of the present theory for the nondimensional standoff distance variation vs Damköhler number for a typical undiluted parametric case, along with results from other theories; following Hornung,[7,11] we have chosen to present these results in terms of the density-scaled standoff ratio

$$\tilde{\Delta} = (\rho_F/\rho_\infty)(\delta_S/2R_B) \tag{16}$$

vs the modified Damköhler number Ω (proportional to Γ_D) defined by

$$\Omega \equiv \theta_F^{N-1} e^{-1/\theta_F}(1-\alpha_\infty) \times \left\{ \frac{1+[2(k_{DA}/k_{DA2})-1]\alpha_\infty + K(k_{Df}/k_{DA2})}{1+\alpha_\infty+K} \right\} \Gamma_D \tag{17}$$

because such presentation has been shown to most efficiently collapse both theory and experiment to a set of universal curves. Bearing in mind some minor differences in details that result in slightly different frozen and equilibrium limit values [namely, the model used for β_S and inclusion of the ambient energy term in Eq. (12)], it is seen that the present approach is in good agreement with Freeman's approximate constant pressure Newtonian shock-layer theory[5] in predicting a significant decrease of $\tilde{\Delta}$ as Ω increases from the very small values pertaining to chemically frozen shock-layer flow ($\Omega \to 0$) to the large values $\Omega \gg 1$ characterizing equilibrium-dissociated flow across the layer. These two predictions in turn are in 15% above, but are otherwise qualitatively similar in trend to the numerical results from Garr and Marrone's CFD Euler program obtained by Hornung,[7] owing to the more exact frozen and equilibrium limits inherent in their program. Further comparison in Fig. 3 with an approximate average-density theory by Hornung and Wen[11] reveals that, in spite of the use of an adjustable constant to ensure matching with the experimental value of the frozen limit standoff distance, this theory differs noticeably from the other three in predicting a much sharper S-shaped curve across the nonequilibrium regime.

The aforementioned suggests that it would be instructive to replot Fig. 3 in terms of the ratio $\tilde{\Delta}/\tilde{\Delta}_F$ vs Ω so as to remove the effect of differences in $\tilde{\Delta}_F$ between the various theories and thus bring out only the relative effect of the nonequilibrium chemistry, which is, in fact, the main object of inquiry. The results are presented in Fig. 4 along with the addition of experimental data points obtained from Ref. 11. It can be seen that except for a small influence of the different near-equilibrium limits all three of the nonempirical theories (including the present one) when viewed on this basis yield virtually the same shape of curve in agreement with experiment, while lying within 5% or less of each other; the Hornung and Wen theory,[11] however, still exhibits a significantly more rapid variation with Ω. The reason for this poorer agreement is thought to be that unlike the three other theories they use an approximate linear density profile, which is only a rough model of the actual profile that results from the effect of a highly nonlinear exponential-temperature-dependent reactive term in the specie conservation equation.

To complete this aspect of our study, comparisons are shown in Fig. 5 with the approximate theory from Stalker[12]; the agreement between his work and the present theory is seen to be good over nearly all of the nonequilibrium-effect regime. Taken

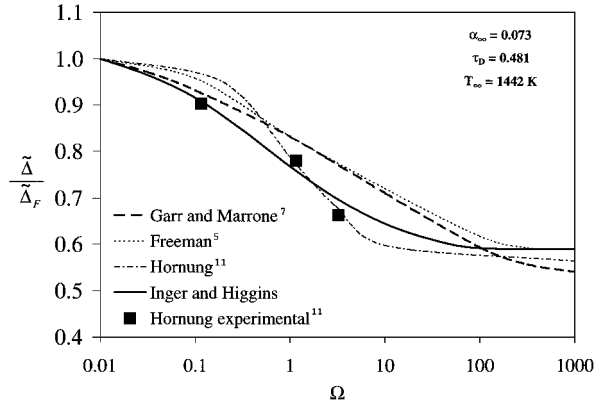

Fig. 4 Correlation of relative shock standoff distance on spheres with reaction-rate parameter for N_2, including experimental data.

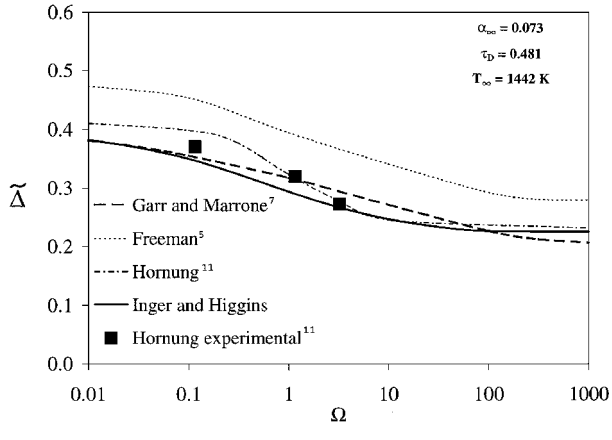

Fig. 3 Typical correlation of density-normalized standoff distance vs reaction-rate parameter for spheres in dissociating N_2.

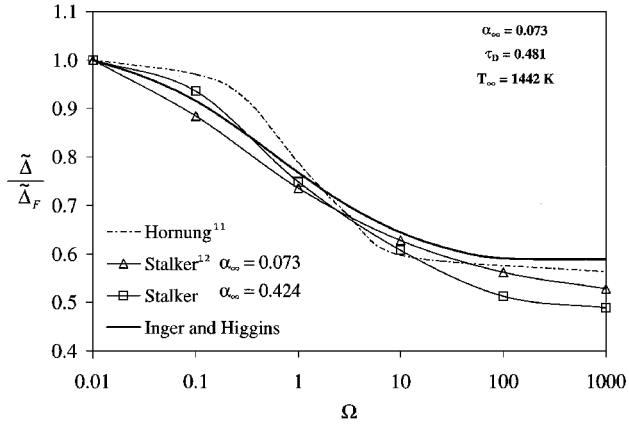

Fig. 5 Comparison of various average-density theories with present analysis (N_2).

in conjunction with the aforementioned comparisons, the present general density-transformation approach is seen to give a good account of all of the significant nonequilibrium chemistry effects on standoff distance as measured by the Damköhler number and hence will serve as a satisfactory basis for assessing the influence of the other similitude parameters noted in Eq. (15).

Freestream Dissociation Effect

The influence of the nonequilibrium freestream dissociation fraction α_∞ on the scaled standoff distance ratio over the entire range of nonequilibrium effect has been assessed using the present theory; a typical result is plotted in Fig. 6. Over a wide range of α_∞ values $0 \le \alpha_\infty \le 0.4$, it is seen that α_∞ has only a small effect on this ratio for much of the nonequilibrium regime up to $\Omega \le 10$. This conclusion is further supported by the numerical results from Garr and Marrone (from Ref. 7), which are in good agreement with the present theory.

Nondimensional Kinetic Energy Parameter τ_D

The similitude parameter τ_D represents the kinetic energy of flight in ratio to the characteristic dissociation energy of the gas in question. In the present work we have for the first time systematically examined the effect of this parameter as shown in Fig. 7. Our present theory predicts that the relative nonequilibrium effect on standoff distance decreases with increasing τ_D throughout the highly nonequilibrium flight regime $\Omega \le 1$, with the standoff distance becoming virtually independent of τ_D for $\tau_D > 1$. This may be understood by examination of the density ratio ρ/ρ_F (which controls the relative nonequilibrium effect on δ_S); from the equations of state and energy, we have $\rho/\rho_F \sim T_F/T \sim \tau_D/[\tau_D - (\alpha - \alpha_\infty)]$, which indicates that because $(\alpha - \alpha_\infty)$ increases with τ_D via the dissociation rate, ρ/ρ_F becomes insensitive to τ_D when $\tau_D > 1$.

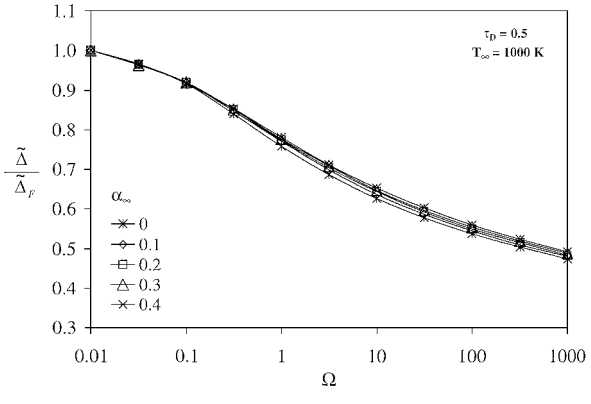

Fig. 6 Freestream dissociation effect on relative nonequilibrium standoff distance for spheres in N_2.

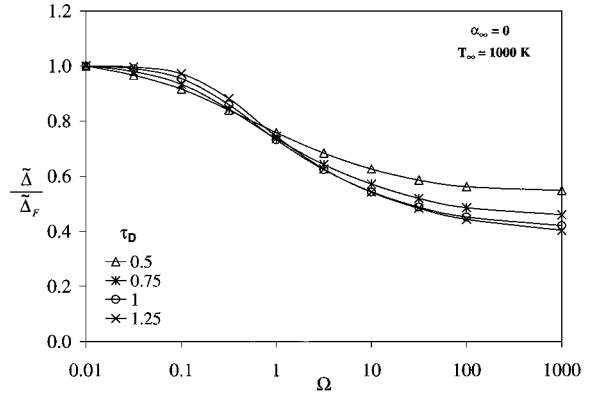

Fig. 7 Influence of the kinetic energy/dissociation energy ratio τ_D on standoff distance for spheres in N_2.

Vibrational/Rotational Energy Activation

Based on the frozen specific heat ratio γ_F immediately behind the shock as a criterion, the present theory predicts that the inclusion of molecular vibrational excitation slightly reduces the relative nonequilibrium effect on standoff distance in nitrogen (Fig. 8a). The comparable influence of including rotational energy excitation in the case of hydrogen, shown in Fig. 8b, is an even greater reduction because more nonequilibrium dissociation occurs when the internal energy modes are unexcited, and hence more of the flight kinetic energy is available for dissociation.

Effect of Inert Dilutent

This effect would be expected to be energetically insignificant and hence a weak influence unless f is close to unity. This is indeed what our results show, as illustrated in Fig. 9: for $f \le 0.70$ the

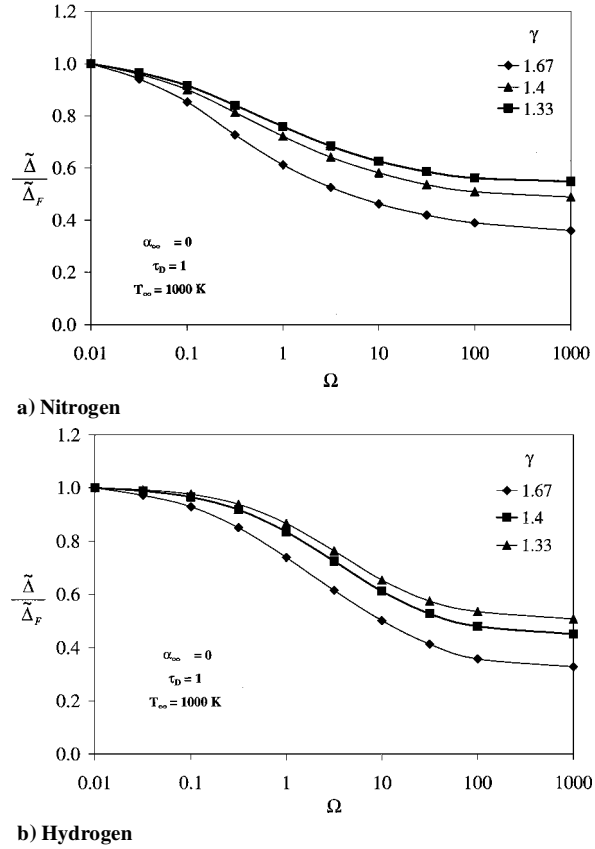

Fig. 8 Influence of molecular internal energy excitation on nonequilibrium standoff distance (spheres).

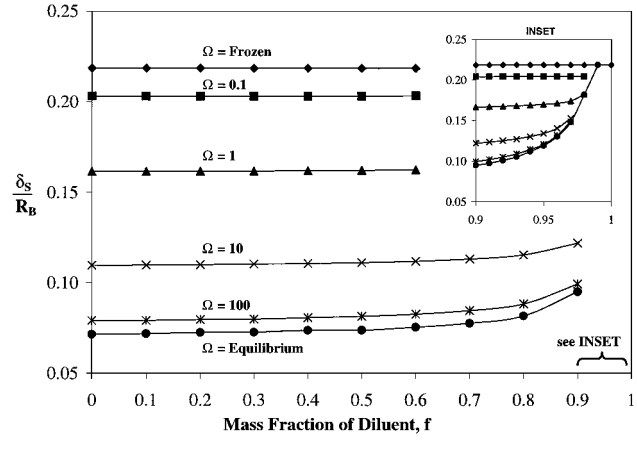

Fig. 9 Influence of dilutent fraction on the nonequilibrium standoff distance for spheres in N_2 (T_∞ = 1000 deg, α_∞ = 0, τ_D = 0.50).

dilution fraction has a negligible effect on the standoff distance over the entire nonequilibrium regime. This conclusion is helpful to the experimentalist because it indicates that the exact amount of dilutent is unimportant. As $f \to 1$ (see insert of Fig. 9), a completely frozen flow is obtained in the shock layer.

Conclusions

The present theory is in good agreement with existing work on undiluted diatomics in showing the expected significant reduction of δ_S as the Damköhler number increases from very small values pertaining to chemically frozen shock-layer flow to the much larger than unity values characterizing equilibrium dissociated flow across the layer. This validation provides encouraging support for our compressibility transformation theory and its future application to more general gas mixtures including multitemperature nonequilibrium ionization.

Acknowledgments

This work was supported by the Australian Research Council, IREX, and the University of Queensland travel scheme.

References

[1]Hornung, H. G., and Smith, G. H., "The Influence of Relaxation on Shock Detachment," *Journal of Fluid Mechanics*, Vol. 93, Pt. 2, 1979, pp. 225–239.

[2]McIntyre, T. J., Wegener, M. J., Bishop, A. I., and Rubinsztein-Dunlop, H., "Simultaneous Two-Wavelength Holographic Interferometry in a Superorbital Expansion Tube Facility," *Applied Optics*, Vol. 36, No. 31, 1997, pp. 8128–8134.

[3]Morgan, R. G., "A Review of the Use of Expansion Tubes for Creating Superorbital Flows," AIAA Paper 97-0279, Jan. 1997.

[4]Stalker, R. J., and Edwards, B. P., "Hypersonic Blunt Body Flows in Hydrogen-Neon Mixtures," AIAA Paper 98-0799, Jan. 1998.

[5]Freeman, N. C., "Non-Equilibrium Flow of an Ideal Dissociating Gas," *Journal of Fluid Mechanics*, Vol. 4, Pt. 3, 1958, pp. 407–425.

[6]Stalker, R. J., "A Similarity Transformation for Blunt-Body Flows," AIAA Paper 86-0125, June 1986.

[7]Hornung, H. G., "Non-Equilibrium Dissociating Nitrogen Flow Over Spheres and Circular Cylinders," *Journal of Fluid Mechanics*, Vol. 53, 1972, pp. 149–176.

[8]Hayes, W. D., and Probstein, R. F., *Hypersonic Flow Theory*, Academic Press, New York, 1959, pp. 150–162.

[9]Gibson, W., "Dissociation Scaling for Nonequilibrium Blunt Nose Flows," *ARS Journal*, Vol. 32, No. 4, 1962, pp. 285–287.

[10]Park, C., "Assessment of Two-Temperature Kinetic Model for Dissociating and Weakly-Ionizing Nitrogen," *Journal of Thermophysics and Heat Transfer*, Vol. 2, No. 1, 1988, pp. 8–16.

[11]Hornung, H. G., and Wen, C. Y., "Non-Equilibrium Dissociating Flow Over Spheres," *Journal of Fluid Mechanics*, Vol. 299, 1995, pp. 389–405.

[12]Stalker, R. J., "Approximation for Nonequilibrium Hypervelocity Aerodynamics," *AIAA Journal*, Vol. 27, No. 12, 1989, pp. 1761–1769.